

Yoo-Jeong Noh* and Guosheng Liu
Florida State University, Tallahassee, FL 32306, USA

1. INTRODUCTION

Many radiative transfer models and physical rain retrieval schemes have an assumption that rain rates are homogeneously distributed across the satellite field of view (FOV). Then, in most cases, we can see significant differences between precipitations derived based on the plane-parallel radiative transfer model and actual observations. The most significant cause for the difference is that precipitations are normally not uniformly distributed within a satellite pixel. This problem has been called the “beamfilling” effect.

The plane-parallel assumption, coupled with the well-known nonlinear response of the brightness temperature, T_b , to precipitation rate (Wilheit et al., 1977) leads to an underestimation of precipitation rates and unrealistic precipitation total, especially when averaging over a long period and a large area. In Fig. 1, the relations between the brightness temperature and surface rainfall rate are shown. The thick line represents the plane-parallel model (Liu and Fu, 2001) result and symbols are derived from the collocated TRMM PR (Precipitation radar) and TMI (TRMM microwave imager) data at 19.4 GHz, horizontal polarization in January 1998 over the Indian Ocean. We can see the differences between the radiative transfer model results and real satellite observations due to the beamfilling effect.

Some previous studies have addressed the problem of inhomogeneous precipitation to rain retrievals (Wilheit et al., 1991; Petty, 1994; Kummerow, 1998). However, there have been no detailed studies on the inhomogeneity of precipitation distribution itself. To more accurately assess the beamfilling effect caused by the inhomogeneity problem of precipitations, it is very important to investigate the characteristics of horizontal precipitation distribution.

In this study, the horizontal inhomogeneity of precipitations from radar data is investigated. Analyses of one-year-long AMeDAS (Automatic Meteorological Data Acquisition System) radar precipitation data around Japan and four-month-long ship borne radar data during TOGA COARE (Tropical Ocean Global Atmosphere Coupled Ocean-

Atmosphere Response Experiment) in the western Pacific Ocean are performed.

2. DATA

2.1 Radar-AMeDAS precipitation data

The AMeDAS (Makihara et al. 1995; Oki et al., 1997) is the name of the network system consisting of an automated operation center and automatic observation stations located all over Japan, linked through a telephone network. The time interval of data acquisition is once per hour. This network includes about 1300 rain gauge stations with a mean spatial interval of 17km. The radar-AMeDAS data are 1-hr accumulated precipitation observations from radars and rain gauges. The data cover all of Japan and its coast area and the spatial resolution is approximately 5km x 5km. The Japan Meteorological Agency produces digital radar-AMeDAS precipitation data and charts routinely for the purpose of short-term rainfall prediction since 1998.

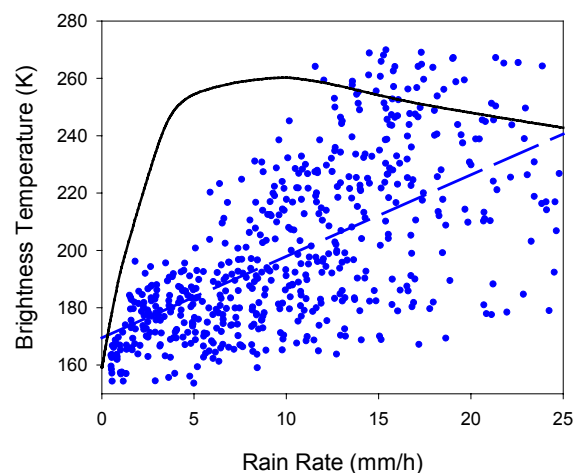


Fig. 1. Brightness temperature as a function of surface rainrate for 19.4 GHz, horizontal polarization. The thick line is derived by the simulations of the MWRT model and symbols by using the collocated TRMM PR and TMI data.

*Corresponding authors address : Yoo-Jeong Noh, Florida State University, Dept. of Meteorology, Tallahassee, FL 32306; e-mail: yjnoh@met.fsu.edu

By integrating eight observations (including two shipborne radars during winter and early summer seasons), 1-hr radar estimated rainfall data are computed. Rain rates observed by radars are adjusted to have the same value at each point in overlapping areas covered by multiple radars and calibrated by the use of AMeDAS rain gauge data.

This estimated 1-hr rainfall database has wide-area and long temporal coverage, preferable for satellite validation studies. The period of the data used in this study is about 13 months from March 2001 to March 2002.

2.2 TOGA COARE data

We also used the four-month TOGA COARE (Lin and Johnson, 1997; Short et al., 1997) radar data. Two 5-cm shipborne radars measured rainfall data every 10 minutes. One was located at 2°S, 154.5°E and the other was at 2°S, 156°E and the period was from 1 November 1992 to 28 February 1993. The gridded rain maps have 2km x 2km resolution.

3. HORIZONTAL DISTRIBUTIONS AND STATISTICS OF PRECIPITATION DATA

The inhomogeneous precipitation distributions are considered within several assumed satellite FOVs. In this study, the pixel sizes corresponding to FOV sizes of 15 km and 25 km for AMeDAS data and 12 km and 24 km for TOGA COARE data are used to analyze precipitation statistics and horizontal distributions. Approximately, the FOV dimension of 12 km is corresponding to the 37 GHz resolution of the TRMM TMI and the 85 GHz resolution of the SSM/I. The 25 km FOV resolution represents the 37 GHz resolution of the SSM/I and the 19 GHz resolution of the TRMM TMI.

To determine the distribution characteristics of rain rate, a large number of pixel-averaged precipitation rates are obtained over the whole domain and entire period of the AMeDAS and the TOGA COARE data sets. According to the averaged precipitation rates, the horizontal distributions are categorized from light precipitation values to heavy ones. Figure 2 shows the probability distributions normalized by the numbers of total pixels in each precipitation range of the AMeDAS rainfall data. It reflects the probability of a certain rain rate at sub-pixel grids given a pixel-averaged rain rate. The shape of the distributions becomes broader as the pixel averaged precipitation rate increases in both 15 km and 25 km (not shown) FOVs. For the TOGA COARE data, the distribution shape is slightly

different, but these aforementioned characteristics are similar.

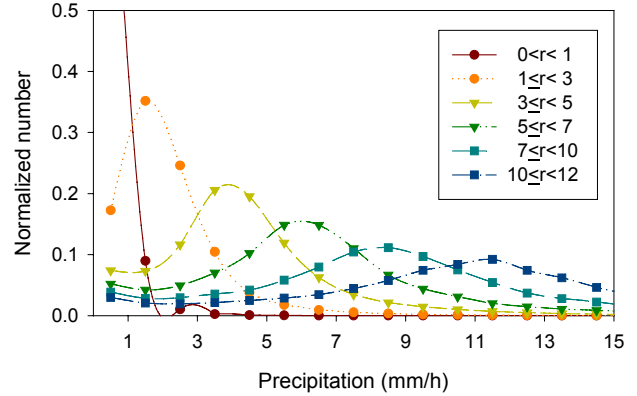


Fig. 2. Probability distribution of precipitation pixels of AMeDAS. FOV is 15 km.

In the present investigation, the statistical characteristics of precipitations are also described. The following statistical parameters (Kummerow, 1998) are determined.

The spatial inhomogeneity of rainfall within the satellite FOV is described by σ_{FOV} :

$$\sigma_{FOV} = \left(\frac{1}{N_{FOV} - 1} \sum_i^{N_{FOV}} (\bar{r} - r_i)^2 \right)^{1/2}, \quad (1)$$

where \bar{r} is the pixel-averaged rainfall rate and N_{FOV} is the number of pixels in the satellite FOV.

The mean inhomogeneity, $\bar{\sigma}_{FOV}$, is the average over the whole domain and all available times.

$$\bar{\sigma}_{FOV} = \frac{1}{M} \sum_i^M \sigma_{FOV}, \quad (2)$$

where M is the total number of radar precipitation time steps. In Table 1, the statistics for precipitation distributions are summarized.

For different FOVs (15km and 25km) of AMeDAS data, $\bar{\sigma}_{FOV}$ s are shown in Fig. 3. As the resolution of FOV becomes higher, this parameter of the mean horizontal inhomogeneity decreases.

It is known that spatially averaged rain rate is highly correlated with the fractional area of rain rates exceeding a preset threshold (Oki et al., 1997). The number of pixels where the rain rates exceeded the value (here, 0 mm/h or 1 mm/h) is counted within a pixel for each averaged precipitation rate. The ratio of the counted number to the total number of pixels is the precipitation fraction. Figure 4 represents the precipitation fractions to the pixel averaged

precipitation rates for two FOVs (15 km and 25 km) of AMeDAS. We can see that the fraction values are different with pixel size (FOV) at weak precipitation rates although the difference is not much at heavy precipitation rates.

Table 1. Precipitation statistics for 15 km FOV of AMeDAS and 12 km FOV of TOGA COARE.

AMeDAS (FOV=15 km)			
Rain Range	\bar{r}	$\bar{\sigma}_{FOV}$	Tot. number of pixels
$0 < r < 1$	0.1015	0.0938	1.65E+08
$1 \leq r < 3$	1.6388	1.0664	22540169
$3 \leq r < 5$	3.884	2.2449	6539301
$5 \leq r < 7$	5.8685	3.1213	3132649
$7 \leq r < 10$	8.3128	4.0818	2408541
$10 \leq r < 12$	10.8967	5.0243	892125
$12 \leq r < 15$	13.3231	5.8517	814175
$15 \leq r < 20$	17.1172	7.0497	675528
$20 \leq r < 50$	26.8758	10.0869	592745
TOGA COARE (FOV=12 km)			
$0 < r < 1$	0.14002	0.272885	72896934
$1 \leq r < 3$	1.707379	2.831653	9277485
$3 \leq r < 5$	3.821554	6.030593	2373452
$5 \leq r < 7$	5.874217	9.187979	950347
$7 \leq r < 10$	8.295642	11.98533	661529
$10 \leq r < 12$	10.92396	14.35853	233914
$12 \leq r < 15$	13.35334	16.36515	208467
$15 \leq r < 20$	17.12379	19.05197	165434
$20 \leq r < 50$	27.14188	27.29921	138802

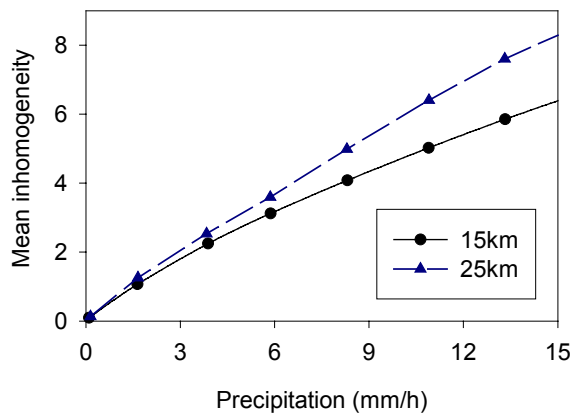


Fig. 3. The difference of the mean inhomogeneity, $\bar{\sigma}_{FOV}$ for 15 km and 25 km FOVs of AMeDAS data.

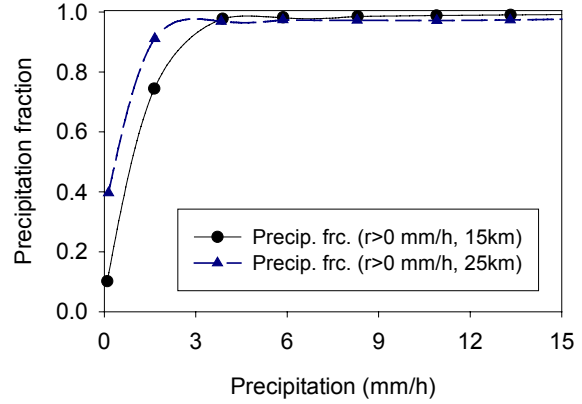


Fig. 4. Precipitation fraction as a function of the pixel averaged precipitation rates for 15 km and 25 km FOVs of AMeDAS data.

In Fig. 5, the precipitation fraction within the sub-pixel is obtained. When a pixel has the averaged rain rate greater than a certain threshold (about 3 mm/h for AMeDAS and about 2 mm/h for TOGA COARE), this fraction, which is the number ratio of rainy to total observations within a satellite pixel, rapidly reaches 1. Also, in this figure, it is found that weak precipitations ($0 \text{ mm/h} < r < 1 \text{ mm/h}$) are dominant, and the averaged precipitation fraction is much smaller during the TOGA COARE period compared with AMeDAS.

4. SUMMARY

In this study, we investigated the horizontal inhomogeneity of precipitations using radar data. Analyses of the characteristics of precipitation distributions and statistical parameters using the AMeDAS radar precipitation data and the TOGA COARE data were performed.

By analyzing the characteristics of precipitation inhomogeneity, we determined the probability distribution functions, which can be usefully applied to rain retrieval schemes to more accurately deal with the beamfilling effect caused by the inhomogeneity problem of precipitations. Furthermore, the study of the seasonal and regional variations for precipitation distribution will provide important basis in the developments of radiative transfer models and retrieval schemes.

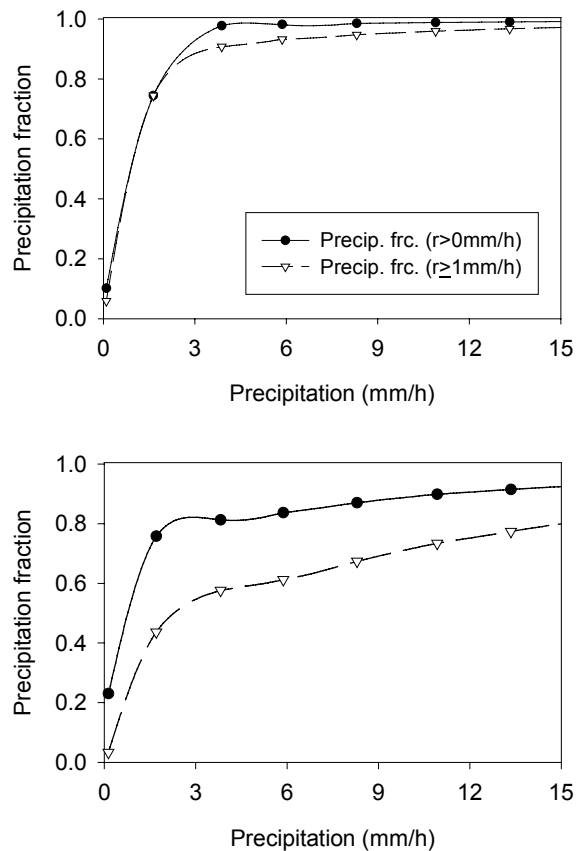


Fig. 5. Precipitation fraction as a function of the pixel averaged precipitation rates. The upper is for AMeDAS (FOV=15 km) and the below is for TOGA COARE (FOV=12 km).

5. REFERENCES

- Kummerow, Christian, 1998: Beamfilling errors in passive microwave rainfall retrievals. *J. Appl. Meteor.*, 37, 356-370.
- Lin, Xin and Richard H. Johnson, 1997: Heating, moistening, and rainfall over the western Pacific warm pool during TOGA COARE. *J. Atmos. Sci.*, 53, 3367-3383.
- Liu, G. and Y. Fu, 2001: The characteristics of tropical precipitation profiles as inferred from satellite radar measurements. *J. Meteor. Soc. Japan*, 79, 131-143.
- Makihara, Yasutaka, Naoko Kitabatake, and Masanori Obayashi, 1995: Recent developments in Algorithms for the JMA nowcasting system Part I: Radar echo composition and radar-AMeDAS precipitation analysis. *Geophys. Mag. Series 2*, 1, 171-204.
- Oki, R., A. Sumi, and D. A. Short, 1997: TRMM sampling of radar-AMeDAS rainfall using the threshold method. *J. Appl. Meteor.*, 36, 1480-1492.
- Petty, G. W., 1994: Physical retrievals of over-ocean rain rate from multi-channel microwave imaging. Part I: Theoretical characteristics of normalized polarization and scattering indices. *Meteor. Atmos. Phys.*, 54, 79-99.
- Short, D. A., P. A. Kucera, B. S. Ferrier, J. C. Gerlach, S. A. Rutledge, and O. W. Thiele, 1997: Shipborne radar rainfall patterns within the TOGA COARE IF. *Bull. Amer. Meteor. Soc.*, 78, 2817-2836.
- Wilheit, T. T., A. T. C. Chang, M. S. V. Rao, E. B. Rodgers, and J. S. Theon, 1977: A satellite technique for quantitatively mapping rainfall rates over the oceans. *J. Appl. Meteor.*, 16, 551-560.
- Wilheit, T. R., A. T. C. Chang, and L. S. Chiu, 1991: Retrieval of monthly rainfall indices from microwave radiometric measurements using probability distribution functions. *J. Atmos. Oceanic Technol.*, 8, 118-136.